Eur. Phys. J. C (2024) 84:896
https://doi.org/10.1140/epjc/s10052-024-13275-7

THE EUROPEAN PHYSICAL JOURNAL C

Regular Article - Theoretical Physics

Quantum metrology of Schwinger effect

Tingting Fan[1], **Qianqian Liu**[1], **Jiliang Jing**[1], **Jieci Wang**[1,2,a]

[1] Department of Physics, and Collaborative Innovation Center for Quantum Effects and Applications, Hunan Normal University, Changsha 410081, Hunan, China
[2] Institute of Interdisciplinary Studies, Hunan Normal University, Changsha 410081, Hunan, China

Received: 3 March 2024 / Accepted: 20 August 2024

Abstract We propose a scheme for the quantum metrology of the Schwinger effect and the dynamics of Gaussian interference power (GIP). The ongoing reliability of the estimation strategy for the probe state prepared in particle–particle modes is demonstrated. Although the GIP sensitively depends on the strength of the external electric field and the transverse momentum, the advantage of quantum parameter estimation is still maintained even in the limit of an infinite electric field and zero transverse momentum. It is shown that the entanglement between the particle–particle modes provides a guarantee for obtaining higher precision for the black-box estimation. In contrast, for the probe state prepared in particle–antiparticle modes, the advantage of quantum parameter estimation can also be ensured even though there is no entanglement in the probe state. Put differently, some non-entanglement quantum correlations play the role of quantum resources in the estimation for particle–antiparticle modes.

1 Introduction

Quantum fluctuations spontaneously produce particle pairs from the vacuum, which is a fascinating phenomenon in quantum field theory. Typical quantum fluctuation induced phenomena include the Unruh effect observed by accelerating detectors [1], the Hawking radiation of black holes [2], and the quantum thermal effect induced by inflationary cosmological perturbations [3]. It is also intriguing that the vacuum may decay into particle–antiparticle pairs under the influence of a strong electromagnetic field, which is a phenomenon known as the Schwinger effect [4–6]. This effect is an important non-perturbative prediction from quantum electrodynamics about the production of particle pairs by high-intensity electric fields [7,8]. However, to observe such an effect, the critical electric field is about 10^{16} V/cm, corresponding to the energy flux density in the focal spot of the laser setup close to 10^{29} W/cm^2. So far, the achievable intensity in large-scale scientific projects under construction and commissioning is about 10^{23} W/cm^2 [9–12]. That is to say, although scientists are exploring higher intensity lasers, it is hard to believe that the Schwinger effect can be experimentally observed in the near future. Therefore, in order to explore the relevant properties of the Schwinger effect, we will explore its properties from the perspective of quantum precision measurement. With the development of technology, when the experimental conditions can approach or even exceed this theoretical threshold, our current findings will be able to guide the experimental design of the Schwinger effect and improve its observational accuracy.

The utilization of quantum resources [13] for precision metrology has been one of the most interesting issues in quantum science and technology [14]. This area explores how quantum systems can be leveraged to achieve measurements with unprecedented accuracy and sensitivity, surpassing the limits of classical techniques. In particular, quantum metrology examines the ways in which quantum entanglement, superposition, and other quantum phenomena can be harnessed to improve measurement precision. The problem of quantum metrology can be viewed as the search for optimal strategies for encoding parameter estimation within the parameter-dependent evolution of probe systems. In recent years, the method of quantum metrology has been employed to enhance the estimation of the Unruh-Hawking effect [15–18], cosmological parameters [19,20], and spacetime parameters of the Earth [21,22]. Girolami et al. introduced a framework for black-box quantum metrology [23]. For the black-box estimation, where the generator of the parameter to be estimated is *priori unknown*, the interferometric power

Tingting Fan and Qianqian Liu contributed equally to this work.

[a] e-mail: jcwang@hunnu.edu.cn (corresponding author)

Published online: 04 September 2024

was introduced to quantify the precision of encoded parameter estimation in the worst-case scenario [23]. It has been demonstrated that interferometric power equals a calculable measure of discord-type quantum correlations for the probe state. Subsequently, Adesso proposed a closed formula of GIP for continuous-variable quantum systems [24]. The GIP specifically characterizes the power of interference effects when Gaussian states are employed, providing a quantitative tool tailored for such systems. These concepts illustrate both the foundational role of interferometric power in parameter estimation under unknown conditions and the specialized adaptation of GIP for continuous-variable quantum systems, reflecting their distinct but related roles in quantum information theory.

In this paper, we propose a scheme for black-box estimation of the Schwinger effect in a continuous-variable system by using Gaussian probe states. The present scheme can be theoretically modeled as a two-arm channel, where one subsystem of the initial state is observed by Alice while the other subsystem in the constant electric field is observed by Bob. Encoded within a black-box device influenced by the electric field are the parameters associated with the two-mode squeezing transformation. When the GIP evolves in an electric field where the Schwinger effect occurs, the evolved GIP contains information about the Schwinger effect. Using the information extracted from the GIP, we can obtain optimal conditions that are more suitable for the generation of particle–antiparticle pairs. We demonstrate the ongoing reliability of the estimation strategy for the probe state prepared in particle–particle modes.

The paper is organized as follows. In Sect. 2, we give a brief description for the Schwinger effect in constant electric field. In Sect. 3 we introduce the scheme of the black-box optical interferometer and the role of the GIP. In Sect. 4, we study the black-box estimation of parameters and the behavior of the GIP in the strong electric field. In the final section, we summarize our results.

2 Schwinger effect for scalar field in constant electric field

We consider a scalar field $\phi(t,x)$ with mass m and charge q, which is coupled with a constant electric field E_0 along the z-direction, the Klein–Gordon equation in the four dimensional Minkowski spacetime is given by

$$[(\partial_\mu - iqA_\mu)(\partial^\mu - iqA^\mu) + m^2]\phi(t,x) = 0, \tag{1}$$

where $A_\mu = (0,0,0,-E_0 t)$.

By solving the Klein–Gordon equation, we can obtain two asymptotic complete sets of mode functions $\{\mu^{in}, v^{in}\}$ and $\{\mu^{out}, v^{out}\}$ [25–27], which can be used to expand the scalar field $\phi(t,x)$

$$\begin{aligned}\phi(t,x) &= \sum_{\mathbf{k}} \left[a_{\mathbf{k}}^{\text{in}}\, \mu^{\text{in}} + b_{\mathbf{k}}^{\text{in}\,\dagger} v^{\text{in}} \right] \\ &= \sum_{\mathbf{k}} \left[a_{\mathbf{k}}^{\text{out}}\, \mu^{\text{out}} + b_{\mathbf{k}}^{\text{out}\,\dagger} v^{\text{out}} \right],\end{aligned} \tag{2}$$

where $\mathbf{k}$ denotes the momentum, $a_{\mathbf{k}}$ is the annihilation operator of the particle, $b_{\mathbf{k}}^\dagger$ is the creation operator of the antiparticle, and the superscripts 'in' and 'out' represent the input and output of the bosonic field which corresponding to the absence and presence of the electric field.

The Bogoliubov transformations between the in-modes and the out-modes are related as [28]

$$\begin{aligned} a_{\mathbf{k}}^{\text{in}} &= \alpha_{\mathbf{k}}^* a_{\mathbf{k}}^{\text{out}} - \beta_{\mathbf{k}}^* b_{\mathbf{k}}^{\text{out}\dagger}, \\ b_{\mathbf{k}}^{\text{in}} &= \alpha_{\mathbf{k}}^* b_{\mathbf{k}}^{\text{out}} - \beta_{\mathbf{k}}^* a_{\mathbf{k}}^{\text{out}\dagger}, \end{aligned} \tag{3}$$

where $\alpha_{\mathbf{k}}$ and $\beta_{\mathbf{k}}$ are Bogoliubov coefficients

$$\alpha_{\mathbf{k}} = \frac{\sqrt{2\pi}}{\Gamma(-\eta)} e^{\frac{-i\pi(\eta+1)}{2}},\ \beta_{\mathbf{k}} = e^{-i\pi\eta}, \tag{4}$$

with $\eta = -\frac{1}{2} - i\frac{\zeta}{2}, \zeta = \frac{m^2+k_\perp^2}{qE_0}$ and the transverse momentum $k_\perp$ is defined by $k_\perp^2 = k_x^2 + k_y^2$. Obviously, the Bogoliubov coefficients satisfy the relations $|\alpha_{\mathbf{k}}|^2 = 1 + e^{-\pi\zeta}$, $|\beta_{\mathbf{k}}|^2 = e^{-\pi\zeta}$ and $|\alpha_{\mathbf{k}}|^2 - |\beta_{\mathbf{k}}|^2 = 1$.

Therefore, the in-vacuum state of each mode can be transformed into a superposition state of the out-modes [27]

$$|0_{\mathbf{k}}, 0_{-\mathbf{k}}\rangle^{\text{in}} = \frac{1}{\alpha_{\mathbf{k}}} \sum_{n=0}^{\infty} \left(\frac{\beta_{\mathbf{k}}^*}{\alpha_{\mathbf{k}}^*} \right)^n |n_{\mathbf{k}}, n_{-\mathbf{k}}\rangle^{\text{out}}, \tag{5}$$

where $|n_{\mathbf{k}}\rangle$ and $|n_{-\mathbf{k}}\rangle$ represent respectively the particle number of mode $\mathbf{k}$ and $-\mathbf{k}$. From Eq. (5) we can see that the presence of the strong electromagnetic field destabilizes the vacuum of the scalar field, which contributes to the creation of particle pairs [6,25–27].

3 Black-box optical parameter estimation and the GIP

Here we introduce the scheme of black-box estimation for the Schwinger effect. The total system includes three subsystems: bosonic mode A observed by Alice in the absence of the electric field, bosonic mode B observed by Bob affected by the Schwinger effect and anti-bosonic mode $\bar{B}$ observed by anti-Bob. As shown in Fig. 1, the setup is modeled as a dual-arm channel, where the estimated parameter ζ is encoded to the right arm. We assume Alice and Bob to share a two-mode squeezed state ρ_{AB}^{in} in Bunch–Davies vacuum, which plays as the probe state at the "in" side. Then the mode B in the right

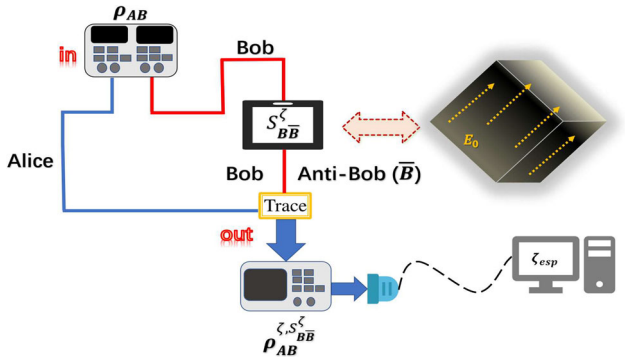

Fig. 1 Two-arm black box quantum parameter estimation scheme. ρ^{in}_{AB} is a two-mode squeezed initial entangled state shared by Alice and Bob, where the mode B in the right arm will pass through the black box device and thus undergo a two-mode squeezing transformation $S^{\zeta}_{B\bar{B}}$ in response to a constant electric field. The mode A in the left arm is unaffected and remains unchanged. The output state $\rho^{\zeta,S^{\zeta}_{B\bar{B}}}_{AB}$ is obtained by tracing over the anti-particle mode $\bar{B}$

arm of the channel is influenced by the vacuum fluctuation of a constant electric field. Due to the Schwinger effect, mode B undergoes a two-mode squeezing transformation $S^{\zeta}_{B\bar{B}}$, which efficiently encodes the estimated parameter ζ. This encoding process, involving the non-prior parameter ζ, is treated as a black-box device. Notably, after the two-mode squeezing transformation, mode B is mapped into two sets of modes: the particle mode B and the antiparticle mode $\bar{B}$. This mapping not only reveals the profound influence of the electric field on the bosonic field state but also provides a rich source of information for subsequent quantum parameter estimation. Meanwhile, the other mode A in the left arm of the channel is not subjected to the electric field. Finally, by tracing over the mode $\bar{B}$, we get the output state $\rho^{\zeta,S^{\zeta}_{B\bar{B}}}_{AB}$ at the "out" side, and one can perform measurements on the output state $\rho^{\zeta,S^{\zeta}_{B\bar{B}}}_{AB}$ to construct an estimator ζ_{esp} for the parameter ζ. The ζ_{esp} is a specific estimator derived from the experimental data and used to estimate the parameter ζ in the experiment. If N measurements are performed independently on the transformed state, the uncertainty of the parameter ζ will be constrained by the Cramér-Rao bound [29,30]

$$\Delta\zeta^2 \geq \frac{1}{N\mathcal{F}(\sigma^{\zeta,S^{\zeta}_{B\bar{B}}}_{AB})}, \tag{6}$$

where $\Delta\zeta^2 \equiv \langle(\zeta_{\text{est}} - \zeta)^2\rangle$ represents the variance of the parameter ζ, and $\mathcal{F}$ at the denominator is quantum Fisher information [30,31]. After performing specific optimized measurements on the output state $\rho^{\zeta,S^{\zeta}_{B\bar{B}}}_{AB}$, the quantum Fisher information quantifies the precision achievable using the input probe state ρ^{in}_{AB}. Therefore, the quantum Fisher information is often considered as a quality factor in quantum metrology.

The GIP of a two-mode Gaussian probe state with covariance matrix $\boldsymbol{\sigma}_{AB}$ is defined as [24]

$$\mathcal{P}^{B}_{G}(\boldsymbol{\sigma}_{AB}) = \frac{1}{4}\inf_{S^{\zeta}_{B\bar{B}}} \mathcal{F}(\boldsymbol{\sigma}^{\zeta,S^{\zeta}_{B\bar{B}}}_{AB}), \tag{7}$$

where $\frac{1}{4}$ is a normalization factor and the elements of the covariance matrix $\boldsymbol{\sigma}_{AB}$ reflect the degree of correlation and the uncertainty between two variables in the quantum state [32]. From Eq. (7) we can know that the GIP $\mathcal{P}^{B}(\boldsymbol{\sigma}_{AB})$ evaluates the minimum quantum Fisher information, which represents the lowest precision that can be obtained among all possible local dynamic choices when ρ_{AB} is used as a probe state and measurements are made from mode B [33]. Moreover, the covariance matrix of the bipartite state ρ_{AB} can always be put into a block form [32]

$$\boldsymbol{\sigma}_{AB} = \begin{pmatrix} \mathcal{A} & \mathcal{C} \\ \mathcal{C}^{\mathsf{T}} & \mathcal{B} \end{pmatrix}, \tag{8}$$

where $\mathcal{A} = \text{diag}(a, a)$, $\mathcal{B} = \text{diag}(b, b)$ and $\mathcal{C} = \text{diag}(c, d)$. In this case, one can obtain a closed formula for the GIP for two-mode Gaussian states [24]

$$\mathcal{P}^{B}_{G}(\boldsymbol{\sigma}_{AB}) = \frac{X + \sqrt{X^2 + YZ}}{2Y}, \tag{9}$$

where

$$X = (I_{\mathcal{A}} + I_{\mathcal{C}})(1 + I_{\mathcal{B}} + I_{\mathcal{C}} - I) - I^2,$$
$$Y = (I - 1)(1 + I_{\mathcal{A}} + I_{\mathcal{B}} + 2I_{\mathcal{C}} + I),$$
$$Z = (I_{\mathcal{A}} + I)(I_{\mathcal{A}}I_{\mathcal{B}} - I) + I_{\mathcal{C}}(2I_{\mathcal{A}} + I_{\mathcal{C}})(1 + I_{\mathcal{B}}),$$

with $I_{\mathcal{A}} = \det\mathcal{A}$, $I_{\mathcal{B}} = \det\mathcal{B}$, $I_{\mathcal{C}} = \det\mathcal{C}$, and $I = \det\boldsymbol{\sigma}_{AB}$.

It is well known that quantum entanglement plays an important role in quantum information theory such as quantum teleportation and quantum communication [34,35]. On the other hand, the dynamics of entanglement contains the information of Schwinger effect in the present scheme. To better understand the role of entanglement in the black-box metrology, we also calculate quantum entanglement in the same state. The measurement of quantum entanglement can be achieved through the logarithmic negativity [13]

$$\varepsilon(\sigma_{AB}) = \max\left\{0, -\log\sqrt{\frac{\Delta - \sqrt{\Delta^2 - 4\det\sigma_{AB}}}{2}}\right\}, \tag{10}$$

where $\Delta = I_{\mathcal{A}} + I_{\mathcal{B}} - 2I_{\mathcal{C}}$. A higher value of logarithmic negativity indicates stronger entanglement. Therefore, loga-

rithmic negativity allows for a quantitative assessment of the entanglement strength in mixed-state quantum systems.

4 Black-box estimation and GIP in the constant electric field

We assume that Alice and Bob initially share a two-mode squeezed vacuum state as the input state, which has the covariance matrix [36,37]

$$\sigma_{AB}(\mathbf{p},\mathbf{q})^{\text{in}} = \begin{pmatrix} \cosh(2s) & 0 & \sinh(2s) & 0 \\ 0 & \cosh(2s) & 0 & -\sinh(2s) \\ \sinh(2s) & 0 & \cosh(2s) & 0 \\ 0 & -\sinh(2s) & 0 & \cosh(2s) \end{pmatrix}, \tag{11}$$

where $\mathbf{p}$ and $\mathbf{q}$ stand for the respective momenta of the two modes observed by Alice and Bob and s is the squeezing parameter of the initial state. As shown in Fig. 1, only Bob's mode is affected by the constant electric field in the present model. From Eq. (5), we can see that the "in" vacuum state $|0_{\mathbf{k}}, 0_{-\mathbf{k}}\rangle^{\text{in}}$ is related with the Fock state $|n_{\mathbf{k}}, n_{-\mathbf{k}}\rangle^{\text{out}}$ by a two-mode squeezing transformation. In the phase space, we use a symplectic operator $S^{\zeta}_{B\bar{B}}(\mathbf{q},-\mathbf{q})$ to express such transformation, which is [37]

$$S^{\zeta}_{B\bar{B}}(\mathbf{q},-\mathbf{q}) = \begin{pmatrix} |\alpha_{\mathbf{q}}| & 0 & |\beta_{\mathbf{q}}| & 0 \\ 0 & |\alpha_{\mathbf{q}}| & 0 & -|\beta_{\mathbf{q}}| \\ |\beta_{\mathbf{q}}| & 0 & |\alpha_{\mathbf{q}}| & 0 \\ 0 & -|\beta_{\mathbf{q}}| & 0 & |\alpha_{\mathbf{q}}| \end{pmatrix}, \tag{12}$$

where ζ is the dimensionless parameter and $S^{\zeta}_{B\bar{B}}(\mathbf{q},-\mathbf{q})$ represents the squeezing transformation performed to the bipartite state shared between Bob and anti-Bob($\bar{B}$). After the action of the transformation, the initial two-body system becomes tripartite. Then we can obtain the covariance matrix $\sigma_{AB\bar{B}}$ of the tripartite quantum system [36,37]

$$\sigma_{AB\bar{B}}(\mathbf{p},\mathbf{q},-\mathbf{q})^{\text{out}} = \big[I_A(\mathbf{p}) \oplus S^{\zeta}_{B\bar{B}}(\mathbf{q},-\mathbf{q})\big[\sigma_{AB}(\mathbf{p},\mathbf{q})^{\text{in}} \oplus I_{\bar{B}}(\mathbf{q})\big]\big[I_A(\mathbf{p}) \oplus S^{\zeta}_{B\bar{B}}(\mathbf{q},-\mathbf{q})\big]^{\mathsf{T}}, \tag{13}$$

where the identity matrix corresponds to the covariance matrix of a vacuum state. The estimation of parameters ζ can be realized by taking measurements in this state. From Eq. (13) we can see that for the initial state $\sigma_{AB}(\mathbf{p},\mathbf{q})^{\text{in}} \oplus I_{\bar{B}}(\mathbf{q})$ mode $\bar{B}$ has no correlation with the bipartite system $\sigma_{AB}(\mathbf{p},\mathbf{q})^{\text{in}}$.

4.1 Black-box parameter estimation using particle–particle modes

The system we study is a three-body system in which the subsystems Alice and Bob are described by the particle modes A and B with momentums $\mathbf{p}$ and $\mathbf{q}$, respectively, and the subsystem anti-Bob is described by the antiparticle model $\bar{B}$ with momentum $-\mathbf{q}$. In this part, firstly, we study the precision of the black-box parameter estimation and quantum entanglement in particle–particle modes. Taking the trace to the anti-Bob mode $\bar{B}$, we obtain the reduced covariance matrix for Alice and Bob

$$\sigma_{AB}(\mathbf{p},\mathbf{q})^{\text{out}} = \begin{pmatrix} \cosh(2s) & 0 & |\alpha_{\mathbf{q}}|\sinh(2s) & 0 \\ 0 & \cosh(2s) & 0 & -|\alpha_{\mathbf{q}}|\sinh(2s) \\ |\alpha_{\mathbf{q}}|\sinh(2s) & 0 & |\alpha_{\mathbf{q}}|^2\cosh(2s)+|\beta_{\mathbf{q}}|^2 & 0 \\ 0 & -|\alpha_{\mathbf{q}}|\sinh(2s) & 0 & |\alpha_{\mathbf{q}}|^2\cosh(2s)+|\beta_{\mathbf{q}}|^2 \end{pmatrix}. \tag{14}$$

The GIP and entanglement of $\sigma_{AB}(\mathbf{p},\mathbf{q})^{\text{out}}$ can be calculated via Eq. (9) and Eq. (10).

In Fig. 2a, we demonstrate the dynamics of the GIP and quantum entanglement for the state $\sigma_{AB}(\mathbf{p},\mathbf{q})^{\text{out}}$ as a function of the external electric field strength E_0. Note that probe states with higher GIP can ensure smaller variance in the black-box parameter estimation. It is shown that the GIP and entanglement between Alice and Bob monotonically decrease as E_0 increases. The more entanglement in the probe state, the higher GIP and precision is obtained in the black-box estimation. This in fact verifies that quantum entanglement is the main resource in estimation of Schwinger effect by using particle–particle modes. Additionally, there is a decrease in the GIP with increasing charge parameter q. This indicates that the measurement precision can be enhanced by reducing charge. Interestingly, even in the limit of the electric field strength E_0 approaches infinity, the GIP maintains non-zero. This highlights the robust nature of the GIP under the influence of the Schwinger effect, indicating the ongoing reliability of the parameter estimation strategy.

In Fig. 2b, we plot the GIP and quantum entanglement as a function of momentum $k_{\perp}$. We can see that both the GIP and entanglement of the probe state are monotonically increasing functions of the transverse momentum $k_{\perp}$. It is note worthy that even as $k_{\perp}$ approaches zero, the GIP maintains non-zero, verifying the ongoing reliability of the black-box parameter estimation strategy. Importantly, we find that the smaller the

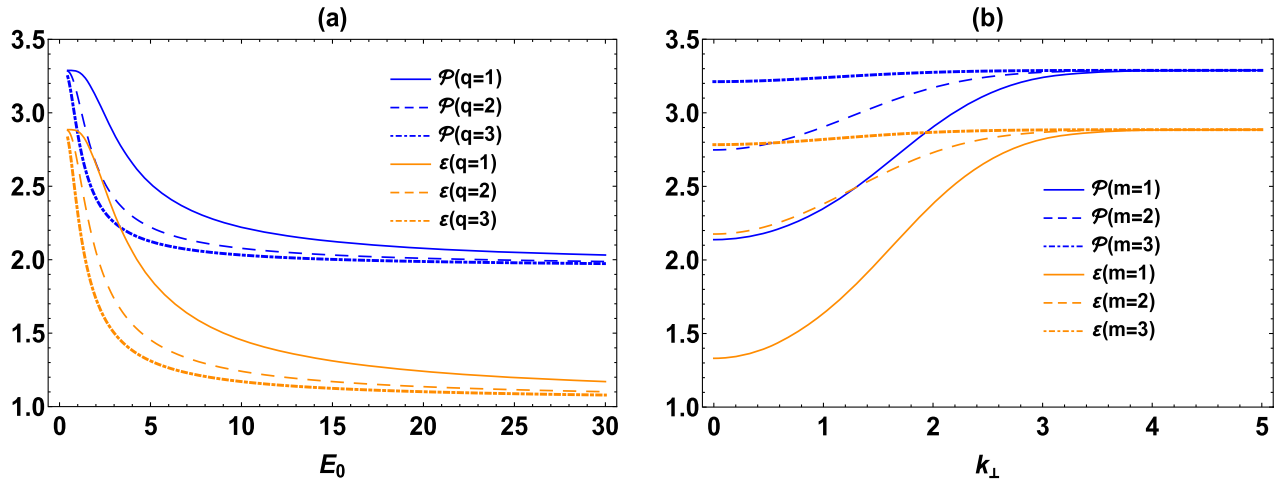

Fig. 2 **a** The GIP ($\mathcal{P}$) and entanglement ε between Alice and Bob as a function of E_0 for fixed values $s, m, k_\perp = 1$. **b** The evolution of the GIP ($\mathcal{P}$) and entanglement ε as a function of $k_\perp$ for fixed values $s, q = 1$ and $E_0 = 7$

bosonic particle mass m is, the more sensitive the GIP and entanglement are to changes in the transverse momentum $k_\perp$, and that a larger bosonic particle mass m is advantageous in enhancing the precision of parameter estimation.

To sum up, the ongoing reliability of the black-box parameter estimation strategy by using particle–particle modes has been demonstrated in Fig. 2a, b. In addition, a higher precision can be achieved by decreasing the strength of the electric field E_0, reducing the charge q, increasing the boson particle mass m, and elevating the momentum $k_\perp$. These factors collectively contribute to obtaining higher precision in the estimation of parameters between the modes of the particles.

4.2 Black-box parameter estimation using particle–antiparticle modes

We are also interested in the precision of the black-box parameter estimation and quantum entanglement by using particle–antiparticle modes. The reduced covariance matrix between Alice and anti-Bob is obtained by tracing over the mode B

$$\sigma_{A\bar{B}}(\mathbf{p},-\mathbf{q})^{\text{out}} = \begin{pmatrix} \cosh(2s) & 0 & |\beta_{\mathbf{q}}|\sinh(2s) & 0 \\ 0 & \cosh(2s) & 0 & |\beta_{\mathbf{q}}|\sinh(2s) \\ |\beta_{\mathbf{q}}|\sinh(2s) & 0 & |\beta_{\mathbf{q}}|^2\cosh(2s)+|\alpha_{\mathbf{q}}|^2 & 0 \\ 0 & |\beta_{\mathbf{q}}|\sinh(2s) & 0 & |\beta_{\mathbf{q}}|^2\cosh(2s)+|\alpha_{\mathbf{q}}|^2 \end{pmatrix}. \tag{15}$$

The GIP and entanglement of state $\sigma_{A\bar{B}}(\mathbf{p},-\mathbf{q})^{\text{out}}$ can be obtained by using this covariance matrix and have been plotted in Fig. 3.

As depicted in Fig. 3, there is no entanglement between Alice and anti-Bob. This is because the Schwinger effect is a local channel, Alice and anti-Bob are initially uncorrelated systems while the Schwinger effect cannot produce entanglement. From Fig. 3a, we find that GIP is a monotonically increasing function of the electric field strength E_0 and maintains a non-zero value when $E_0 \longrightarrow \infty$. It is also shown that higher accuracy in parameter estimation can be achieved by employing particles with larger charges. These results suggest that a higher GIP represents more reliable quantum resources for the quantum metrology process, even in scenarios where the entanglement between Alice and anti-Bob is zero. The Schwinger effect may produce some non-entanglement quantum resources between Alice and anti-Bob. In other words, the role of quantum resources for the black-box estimation is played by non-entanglement quantum correlation, i.e., the discord-type correlation. As illustrated in Fig. 3b, the GIP exhibits a monotonically decreasing with respect to the transverse momentum $k_\perp$. A smaller value of $k_\perp$ corresponds to a higher accuracy in parameter estimation, with the best estimation precision achieved at $k_\perp = 0$. Finally, we find that a smaller mass m of the bosonic particles is beneficial for improving the precision of estimation.

Finally, we discuss the behavior of the GIP between Bob and anti-Bob. The covariance matrix $\sigma_{B\bar{B}}(\mathbf{q},-\mathbf{q})^{\text{out}}$ is obtained by tracing off the mode A

$$\sigma_{B\bar{B}}(\mathbf{q},-\mathbf{q}) = \begin{pmatrix} \mathcal{A}_{\mathbf{q},-\mathbf{q}} & \mathcal{C}_{\mathbf{q},-\mathbf{q}} \\ \mathcal{C}^{\mathsf{T}}_{\mathbf{q},-\mathbf{q}} & \mathcal{B}_{\mathbf{q},-\mathbf{q}} \end{pmatrix}, \tag{16}$$

where

$$\mathcal{A}_{\mathbf{q},-\mathbf{q}} = [|\alpha_{\mathbf{q}}|^2\cosh(2s)+|\beta_{\mathbf{q}}|^2]I_2,$$
$$\mathcal{B}_{\mathbf{q},-\mathbf{q}} = [|\beta_{\mathbf{q}}|^2\cosh(2s)+|\alpha_{\mathbf{q}}|^2]Z_2,$$

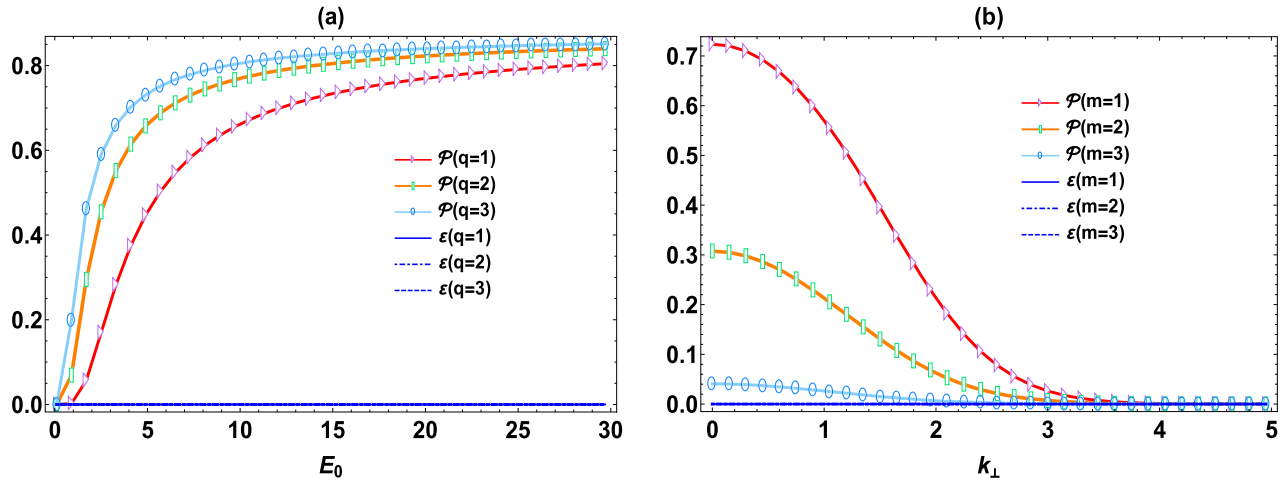

Fig. 3 **a** Plots of the GIP ($\mathcal{P}$) and entanglement ε for the probe state $\sigma_{A\bar{B}}(\mathbf{p}, -\mathbf{q})^{\text{out}}$ as a function of E_0 for fixed values $s, m, k_\perp = 1$. **b** Plots of the GIP ($\mathcal{P}$) and entanglement ε as a function of $k_\perp$ for fixed values $s, q = 1$ and $E_0 = 7$

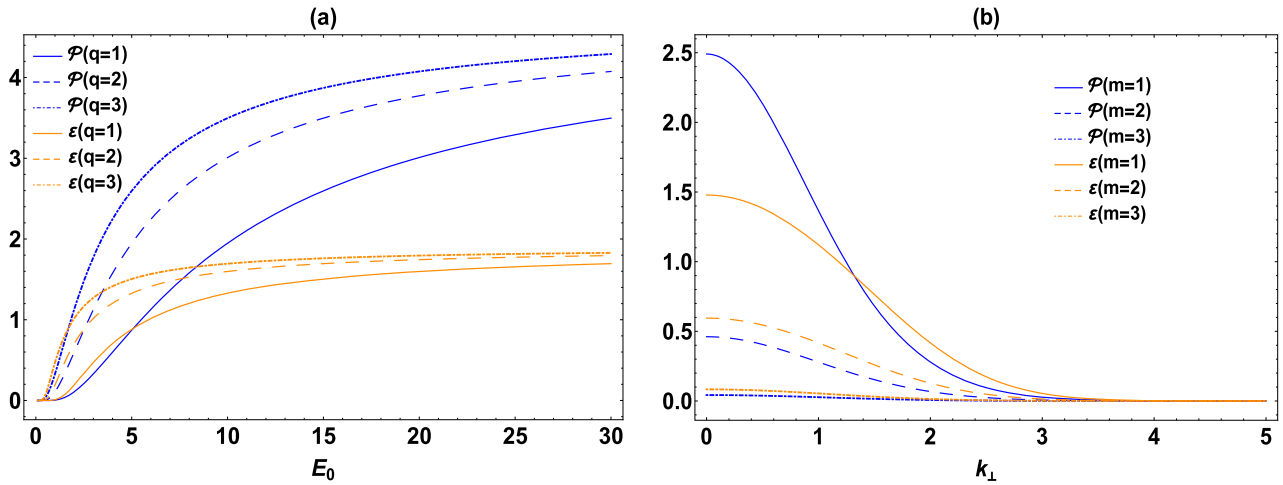

Fig. 4 **a** Plots of the GIP ($\mathcal{P}$) and entanglement ε for the probe state $\sigma_{B\bar{B}}(\mathbf{q}, -\mathbf{q})^{\text{out}}$ as a function of E_0 for fixed values $s, m, k_\perp = 1$. **b** Plots of the GIP ($\mathcal{P}$) and entanglement ε as a function of $k_\perp$ for fixed values $s, q = 1$ and $E_0 = 7$

$$\mathcal{C}_{\mathbf{q},-\mathbf{q}} = 2|\alpha_{\mathbf{q}}||\beta_{\mathbf{q}}|\cosh^2(s)Z_2,$$

and I_2 and Z_2 are Pauli operators. Similarly, the GIP and entanglement between Bob and anti-Bob can be calculated by employing the measurements introduced above.

In Fig. 4, we plot the behavior of the GIP and entanglement between Bob and anti-Bob. It is shown that the GIP between Bob and anti-Bob exhibits an increasing trend as the electric field strength E_0 increases, following the same trend as the entanglement. Notably, with increasing the strength E_0, the bipartite entanglement between Bob and anti-Bob first increases and then demonstrates an asymptotic value, while the entanglement between Alice and anti-Bob remains zero. This observation suggests that quantum entanglement can be generated between Bob and anti-Bob under the influence of the Schwinger effect, serving as the crucial resource for the black-box parameter estimation. Then we can conclude that the precisions of parameter estimation between particle–antiparticle modes are influenced by several parameters. Specifically, a higher precision can be achieved by increasing the strength of the electric field E_0, increasing the charge q, decreasing the boson particle mass m and the transverse momentum $k_\perp$.

5 Conclusion

In this paper, we propose a black-box quantum parameter estimation scheme for the Schwinger effect. The results show that quantum entanglement provides a guarantee for obtaining higher precision for the estimation using particle–particle modes. It is found that although the GIP and entanglement of the probe state sensitively depend on the strength

of the external electric field and the transverse momentum, the advantage of quantum parameter estimation still remains even in the limit of the infinite electric field and zero transverse momentum. Notably, the benefits of quantum metrology persist when there is no entanglement between particle–antiparticle modes, with discord-type correlations fulfilling the role of quantum resources in black-box parameter estimation under these circumstances. Furthermore, the GIP exhibits robust behavior with respect to the strength of the electric field, which ensures the ongoing reliability of the black-box parameter estimation strategy. In addition, for particle–particle modes, a higher accuracy in parameter estimation can be achieved by reducing the strength of the electric field, increasing the mass, transverse momentum, and decreasing the charge of the bosonic particles. For particle–antiparticle modes, increasing the strength of the electric field, decreasing the mass, transverse momentum, and increasing the charge of the bosonic particles are effective strategies to improve the estimation accuracy.

Finally, we need to point out that our work is based on quantum theoretical studies and aims to explore the properties of the Schwinger effect from the perspective of quantum information. We have reason to believe that in the distant future, when the experimental conditions are gradually approaching or even exceeding the theoretical threshold for realizing the Schwinger effect, the results of our current research will not only be able to guide the experimental design and improve the observational precision, but may also be directly applied to the frontier field of quantum information processing, and push forward the significant progress in quantum science and technologies.

Acknowledgements This work is supported by the National Natural Science Foundation of China under Grant No. 12122504, No.12203009, No.12374408 and No. 12035005; the innovative research group of Hunan Province under Grant No. 2024JJ1006; and the Natural Science Foundation of Hunan Province under grant No. 2023JJ30384.

Data Availability Statement This manuscript has no associated data. [Authors' comment: Data sharing not applicable to this article as no datasets were generated or analysed during the current study].

Code Availability Statement This manuscript has no associated code/software. [Author's comment: Code/Software sharing not applicable to this article as no code/software was generated or analysed during the current study].

Funded by SCOAP[3].

References

1. W.G. Unruh, Phys. Rev. D **14**, 870 (1976)
2. S.W. Hawking, Commun. Math. Phys. **43**, 199 (1975)
3. J. Martin, Lect. Notes Phys. **738**, 193 (2008)
4. F. Sauter, Z. Phys. **69**, 742 (1931)
5. W. Heisenberg, H. Euler, Z. Phys. **98**, 714 (1936)
6. J. Schwinger, Phys. Rev. **82**, 664 (1951)
7. S. Kaushal, Eur. Phys. J. C **82**, 872 (2022)
8. R.L.J. Costa, R.F. Sobreiro, Eur. Phys. J. C **82**, 677 (2022)
9. J.P. Zou et al., High Power Laser Sci. Eng. **3**, e2 (2015)
10. S. Weber et al., Matter Rad. Extremes **2**, 149 (2017)
11. N.V. Zamfir, Eur. Phys. J. Spec. Top. **223**, 1221 (2014)
12. J.H. Sung et al., Opt. Lett. **42**, 2058 (2017)
13. W.K. Wootters, Phys. Rev. Lett. **80**, 2245 (1998)
14. V. Giovannetti, S. Lloyd, L. Maccone, Nat. Photon. **5**, 222 (2011)
15. M. Aspachs, G. Adesso, I. Fuentes, Phys. Rev. Lett. **105**, 151301 (2010)
16. D. Hosler, P. Kok, Phys. Rev. A **88**, 052112 (2013)
17. M. Ahmadi, D.E. Bruschi, I. Fuentes, Phys. Rev. D **89**, 065028 (2014)
18. J. Wang, L. Zhang, S. Chen, J. Jing, Phys. Lett. B **802**, 135239 (2020)
19. L. Xiao, C. Wen, J. Jing, J. Wang, Eur. Phys. J. C **82**, 684 (2022)
20. H. Du, R.B. Mann, JHEP **05**, 112 (2021)
21. D.E. Bruschi, A. Datta, R. Ursin, T.C. Ralph, I. Fuentes, Phys. Rev. D **90**, 124001 (2014)
22. S.P. Kish, T.C. Ralph, Phys. Rev. D **99**, 124015 (2019)
23. D. Girolami et al., Phys. Rev. Lett. **112**, 210401 (2014)
24. G. Adesso, Phys. Rev. A **90**, 022321 (2014)
25. Y. Li, Y. Dai, Y. Shi, Phys. Rev. D **95**, 036006 (2017)
26. Y. Li, Q. Mao, Y. Shi, Phys. Rev. A **99**, 032340 (2019)
27. Z. Ebadi, B. Mirza, Ann. Phys. **351**, 363 (2014)
28. S.P. Kim, H.K. Lee, Y. Yoon, Phys. Rev. D **78**, 105013 (2008)
29. H. Cramér, *Mathematical Methods of Statistics* (Princeton University, Princeton, 1946)
30. S.L. Braunstein, C.M. Caves, Phys. Rev. Lett. **72**, 3439 (1994)
31. M.G.A. Paris, Int. J. Quantum Inf. **07**, 125 (2009)
32. C. Weedbrook et al., Rev. Mod. Phys. **84**, 621 (2012)
33. D. Girolami et al., Phys. Rev. Lett. **112**, 210401 (2014)
34. C.H. Bennett, G. Brassard, C. Crépeau, R. Jozsa, A. Peres, W.K. Wootters, Phys. Rev. Lett. **70**, 1895 (1993)
35. J.L. Dodd, M.A. Nielsen, M.J. Bremner, R.T. Thew, Phys. Rev. A **65**, 040301 (2002)
36. G. Adesso, S. Ragy, D. Girolami, Class. Quantum Gravity **29**, 224002 (2012)
37. G. Adesso, Phys. Rev. A **76**, 062112 (2007)